JOURNAL OF MATERIALS SCIENCE 23 (1988) 1779–1785

Hydrogen substitution in lithium-aluminosilicates

G. MÜLLER, M. HOFFMANN*, R. NEEFF‡
Institut für Mineralogie, TH Darmstadt, FRG

Quartz and keatite are SiO_2 polymorphs with relatively dense frameworks containing small voids. Aluminosilicates with small charge compensating cations such as lithium, magnesium and zinc can adopt the same types of structures with the cations occupying the voids. It is shown that the lithium content in both quartz- and keatite-type (Li, $Mg_{0.5}$, $Zn_{0.5}$)$AlSi_2O_6$ solid solutions can be ion exchanged against hydrogen from hot concentrated H_2SO_4. This ion exchange can be reversed. At high temperatures water can irreversibly be driven off the hydrogen forms. Neither ion exchange nor thermal dehydration affects space group symmetry or framework linkage, but lattice parameter variations indicate considerable framework distortions. Thermal expansion also varies strongly with cation content. The data indicate that during dehydration aluminium ions leave the framework and enter the voids thereby providing charge compensation for the remaining framework aluminium content.

1. Introduction

Lithium-aluminosilicates with keatite-(β-spodumene) or high-quartz-type structures form extensive solid solutions on the $LiAlSiO_4$–SiO_2 join in the Li_2O–Al_2O_3–SiO_2 system. Because of their abnormally low thermal expansion that is utilized in glass-ceramics, they have been the object of numerous studies. The lithium ions which occupy voids in the (Al, Si)O_2 framework and balance its charge, have rather large mobilities making some members of the series, like β-eucryptite, fast ionic conductors. In the keatite group of solid solutions the lithium ions can be leached out and replaced by hydrogen by the action of hot concentrated acids. This process was originally developed [1] for lithium extraction from suitable lithium ores and has subsequently been applied by Grossman and Lanning [12] to glass-ceramics in order to improve the stability of these materials against high-temperature corrosion. Ostroushko *et al.* [3] also studied the leaching and subsequent dehydration process of β-spodumene and characterized the products by infrared spectroscopy. They found that at temperatures over 700° C lithium ions from Li_2SO_4 can be re-exchanged with hydrogen.

The aim of the study reported here was to provide information on the kinetics of the leaching process in keatite and related solid solutions and on the crystallography of the resulting products.

2. Experimental procedures

2.1. Preparation of materials

From the broad solid solution series between $LiAlSiO_4$ and SiO_2 the composition $LiAlSi_2O_6$ was selected as the base composition for the present investigation mainly for two reasons: compositions poorer in SiO_2 such as $LiAlSiO_4$ decompose in hot concentrated acids and are therefore unsuitable for leaching experiments. In addition, with $LiAlSi_2O_6$, phases of both keatite- and β-quartz-type structure are readily accessible through crystallization of glasses and have been studied in detail previously [4–6], and partial (in keatite-phases) or complete (in β-quartz-phases) substitution of Li^+ by $Mg^{2+}_{0.5}$ or $Zn^{2+}_{0.5}$ is well documented for this or similar compositions [7–11].

Glasses of appropriate composition have been melted from reagent-grade oxides and carbonates in quantities ranging from 50 to 200 g in platinum crucibles. The composition of the glasses has been checked by X-ray fluorescence and atomic absorption analysis. Deviations from normal composition were found to be within 3 rel. % for Li_2O and within 1 rel. % for all other components.

Table I lists the compositions investigated, the melting temperature and times of the glasses and the crystallization conditions for the quartz and keatite phases.

The glasses were quenched in water and subjected to crystallization as-quenched (cullet of typically 1 to 5 mm) or after grinding (to sieve sizes smaller than 60 μm). Crystallization started from the surface and yielded polycrystalline aggregates. Monocrystalline fragments suitable for X-ray studies could also be found occasionally.

2.2. Leaching experiments

Leaching experiments were made in concentrated H_2SO_4 (98%) in a round bottom flask fitted with a reflux condenser. Leaching temperatures varied

Present address: Max-Planck-Institut für Metallforschung, Stuttgart, FRG.
‡*Present address*: Zentrales Forschungslaboratorium, Brown-Boveri AG, Heidelberg, FRG.

0022–2461/88 $03.00 + .12

TABLE I Compositions and heat-treatments

No.	Composition	Melting		Crystallization (β-quartz)		Crystallization (keatite)	
		Time (h)	Temp. (° C)	Time (h)	Temp. (° C)	Time (h)	Temp. (° C)
1	$LiAlSi_2Si_2O_6$	2.5	1550	5	750	3	1200
2	$Mg_{0.2}Li_{0.6}AlSi_2O_6$	2.5	1550	3	800	3	1200
3	$Zn_{0.2}Li_{0.6}AlSi_2O_6$	2.5	1550	3	800	0.3	1100
4	$Mg_{0.5}AlSi_2O_6$	2.5	1550	5	900		
5	$Zn_{0.5}AlSi_2O_6$	4	1630	8	850		

between 200 and 300° C with leaching times from 2 to 116 h. Typically 50 g H_2SO_4 were reacted with 5 g of solids. After leaching, the solids were filtered off, repeatedly rinsed with deionized water and then dried at 130° C.

2.3. Electrolysis and weight loss studies

In order to check reversibility of the substitution, pressed pellets of the hydrogen-containing phases were electrolysed between LiCl electrodes at 200 to 300° C with a d.c. voltage of 300 V (pellet diameter 10 mm, thickness 0.3 mm). Reversibility by diffusion was also checked by immersion of $HAlSi_2O_6$ powders in molten $LiNO_3$, 300° C, 5 h.

Thermal weight loss was determined by repeated firing in air at a series of increasing temperatures and in some runs by thermogravimetry (Netzsch STA 409/429).

2.4. X-ray analysis

X-ray diffractometry (Cu$K\alpha$-radiation) was used to identify the reaction products. Lattice constants were determined by least-squares analysis of powder diffraction diagrams assuming identical space group symmetry as in the lithium-containing starting phases. The results were confirmed by single-crystal work which will be reported elsewhere.

Thermal expansion data were measured on a Guinier–Simon camera equipped with a Johannson-monochromator (Rich. Seifert). In some runs an X-ray diffractometer system equipped with a graphite heating element and a position sensitive proportional counter (Stoe and Co. STADI/P) was also used. As thermal dehydration of the hydrogen-containing phases interferes with thermal expansion, the high-speed data collection of this X-ray system proved particularly valuable.

2.5. Electron microscopy and microanalysis

Morphological and analytical information was obtained in a scanning electron microscope equipped with a detector for energy dispersive X-ray micro-analysis (Philips EM 505, with EDAX-Spectrometer). Quantitative data were derived from comparison with mineral standards (Astimex).

3. Results

3.1. The leaching process

Table II shows analytical results obtained before and after leaching in concentrated hydrosulphuric acid. It is evident that the leaching process has removed virtually all of the Li_2O content, whereas the MgO and ZnO contents remain essentially unchanged. The results on keatite solid solutions are in agreement with the observations of Ostroushko *et al.* [3] that the Li_2O content can be completely removed by acid treatment.

As can be seen in Table II, β-quartz solid solutions of identical compositions show the same behaviour. The fact that the divalent ions Mg^{2+} and Zn^{2+} cannot be removed is probably related to their mobility which is much smaller than that of the lithium ions. Beall *et al.* [12] reported that at higher temperatures (800 to 900° C) Mg^{2+} ions in β-quartz solid solutions can be exchanged against Li^+ ions from molten lithium salts without a collapse of the aluminosilicate framework. It is possible, therefore, that at higher temperatures, leaching of the divalent ions might also occur. Consequently, the products obtained after sufficient leaching in acid (Table II) can be considered to have the stoichiometric formula $HAlSi_2O_6$ and $H_x(Mg, Zn)_{0.5-x/2}AlSi_2O_6$, respectively. The dehydrated forms, if assumed still to have $(Al, Si)_2O_6$ framework structures, can then be represented as $Al_{0.27}[Al_{0.82}Si_{2.18}O_6]$ and $(Mg, Zn)_{0.21}Al_{0.16}[Al_{0.90}Si_{2.10}O_6]$, respectively.

3.2. Dehydration

A typical weight loss curve of an $HAlSi_2O_6$ keatite sample leached at 200° C for 6 h is shown in Fig. 1. The initial weight loss up to about 100° C of ~0.3% is assumed to be due to absorbed water. Then there is a further gradual loss of ~0.5% up to 400° C followed

TABLE II Cation analysis (AAS) (wt %) before and after leaching

	Li_2O	MgO	ZnO
$LiAlSi_2O_6$, keatite	3.65	–	–
keatite, leached 8 h at 250° C	< 0.01	–	–
$LiAlSi_2O_6$, β-quartz	3.70	–	–
β-quartz, leached 8 h 250° C	0.02	–	–
$Mg_{0.2}Li_{0.6}AlSi_2O_6$, keatite	2.15	2.50	–
keatite, leached 116 h 200° C	< 0.01	2.35	–
$Zn_{0.2}Li_{0.6}AlSi_2O_6$, keatite	1.75	–	5.80
keatite, leached 8 h 250° C	0.05	–	5.70

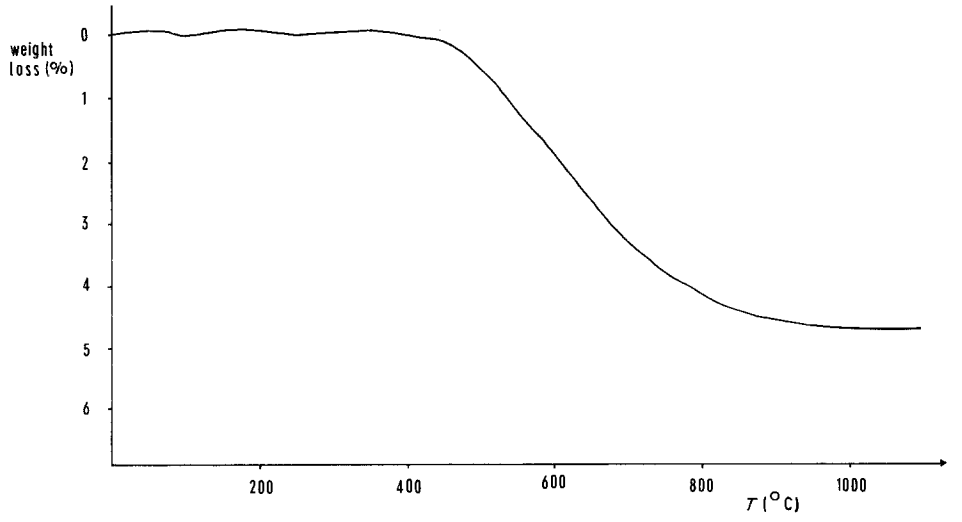

Figure 1 Thermal weight loss of $HAlSi_2O_6$-keatite on heating in air. Heating rate 1.5 K min^{-1}.

by an additional ~4.5% loss until a constant weight is reached at 800 to 900° C.

The total weight loss in the 100 to 900° C range is ~5%. The same result was obtained with isothermal heat treatments at 400, 600 and 800° C: total weight losses (after previous drying at 100° C) were 5.25%, 5.30%, and 5.02%. Constant weight was reached after ~5, 3 and 1 h, respectively.

The weight losses observed are in agreement with the model of Grossmann and Lanning [2] and Ostroushko *et al.* [3]. They assumed that the acid treatment leads to an ion exchange according to the reaction

$$2\ LiAlSi_2O_6 + H_2SO_4 \rightarrow 2\ HAlSi_2O_6 + Li_2SO_4 \quad (1)$$

Full dehydration of $HAlSi_2O_6$ according to the reaction

$$HAlSi_2O_6 \rightarrow AlSi_2O_{5.5} + \tfrac{1}{2}H_2O \quad (2)$$

would require a stoichiometric weight loss of 4.999%, close to the observed amounts. Incorporation of other, heavier molecular species in stoichiometric amounts such as H_3O^+ can be clearly ruled out, apart from the fact that neither the keatite nor the β-quartz structure have voids capable of accommodating molecules or ions having radii larger than ~0.08 nm [4, 5].

3.3. X-ray results: lattice constants and thermal expansion

Space group, lattice constants and structures of $LiAlSi_2O_6$ in the keatite and β-quartz forms are well known [4–6]. For the hydrogen substituted equivalents, as well as the dehydrated forms, no crystallographic data have been published. Similarities in the diffraction diagrams of the lithium, hydrogen and dehydrated forms are obvious and are particularly pronounced in compositions including magnesium or zinc ions, due to the fact that in these cases there is less total compositional change during leaching and dehydration than with pure $LiAlSi_2O_6$ as starting material. This led to the assumption that the space group symmetry is not affected by the leaching and dehydration processes. Indeed the powder diffraction data of all phases could be unambiguously indexed on this basis. The correctness of space group and lattice constants for the $HAlSi_2O_6$ forms is also confirmed by single crystal work that is to be reported elsewhere.

Results of least-squares refinements of the lattice constants of the various forms are given in Table III.

TABLE III Space group, lattice constants and thermal expansion of keatite and β-quartz phases

	keatite-phases, S.G. $P4_32_12$				β-quartz-phases S.G. $P6_222$			
	a_0 (nm)	c_0 (nm)	α_a* ($10^{-6}K^{-1}$)	α_c* ($10^{-6}K^{-1}$)	a_0 (nm)	c_0 (nm)	α_a* ($10^{-6}K^{-1}$)	α_c* ($10^{-6}K^{-1}$)
$LiAlSi_2O_6$	0.7545(4)	0.9156(4)	−3.0(5)	7.9(5)	0.5215(3)	0.5457(3)	1.0(5)	−6.3(5)
$HAlSi_2O_6$	0.7593(4)	0.8408(4)	3.2(8)	10.7(8)	0.5083(3)	0.5509(3)	8.8(8)	−1.7(8)
$Al_{0.27}[Al_{0.82}Si_{2.18}O_6]$	0.7493(8)	0.8842(8)	1.5(7)	3.9(7)	0.5113(5)	0.5434(5)	1.3(7)	−0.7(7)
$Mg_{0.2}Li_{0.6}AlSi_2O_6$	0.7539(4)	0.9163(4)	−0.5(5)	5.5(5)	0.5202(3)	0.5409(3)	3.2(5)	0.0(5)
$Mg_{0.2}H_{0.6}AlSi_2O_6$	0.7528(4)	0.8720(4)	5.0(8)	11.0(8)	0.5115(3)	0.5458(3)	6.0(8)	−0.5(8)
$Mg_{0.21}Al_{0.16}[Al_{0.9}Si_{2.10}O_6]$	0.7501(8)	0.8972(8)	2.8(7)	4.5(7)	0.5154(5)	0.5400(5)	2.5(7)	0.0(7)
$Zn_{0.2}Li_{0.6}AlSi_2O_6$	0.7547(9)	0.9156(4)	−3.8(5)	4.7(5)	0.5216(3)	0.5458(3)	−0.5(5)	−5.0(5)
$Zn_{0.2}H_{0.6}AlSi_2O_6$	0.7542(4)	0.8746(4)	3.2(8)	10.4(8)	0.5127(3)	0.5488(3)	4.1(8)	−2.0(8)
$Zn_{0.21}Al_{0.16}[Al_{0.9}Si_{2.10}O_6]$	0.7525(8)	0.9000(8)	−1.0(7)	5.6(7)	0.5165(5)	0.5440(5)	0.7(7)	−1.2(7)
$Mg_{0.5}[AlSi_2O_6]$					0.5171(5)	0.5343(5)	2.7(5)	1.3(5)
$Zn_{0.5}[AlSi_2O_6]$					0.5220(5)	0.5460(5)	−0.5(7)	−6.0(7)

*Temperature range 25 to 350° C for hydrogen containing phases, 25 to 800° C for all others.

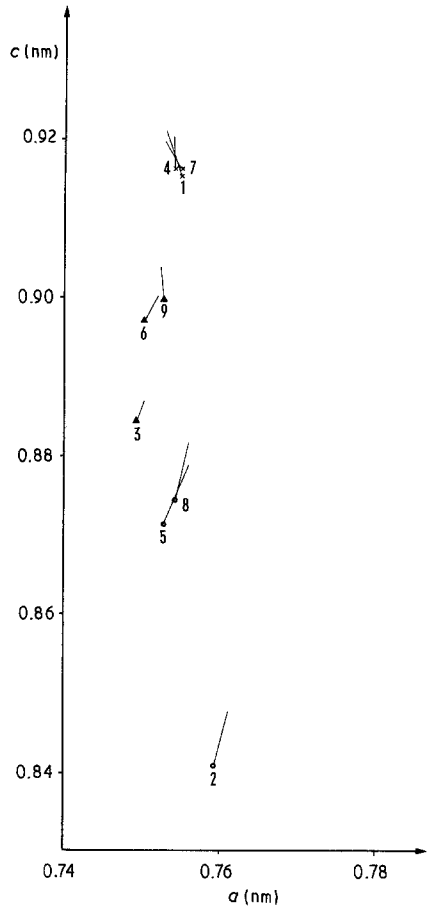

Figure 2 Lattice constants and thermal expansion of keatite phases. Thermal expansion is normalized to 20 to 800° C range and given by lines extending from room-temperature data points. Numbers specify cation charge balance of $(Al, Si)_2O_6$ framework: 1, Li; 2, H; 3, $Al_{0.27}$; 4, $Mg_{0.2}Li_{0.6}$; 5, $Mg_{0.2}H_{0.6}$; 6, $Mg_{0.21}Al_{0.16}$; 7, $Zn_{0.2}Li_{0.6}$; 8, $Zn_{0.2}H_{0.6}$; 9, $Zn_{0.21}Al_{0.16}$.

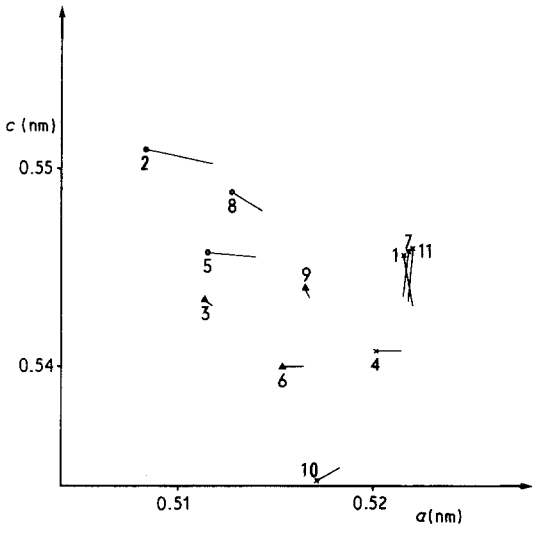

Figure 3 Lattice constants and thermal expansion of β-quartz phases. Thermal expansion is normalized to 20 to 800° C range and given by lines extending from room-temperature data points. Numbers specify cation charge balance of $(Al, Si)_2O_6$ framework: 1, Li; 2, H; 3, $Al_{0.27}$; 4, $Mg_{0.2}Li_{0.6}$; 5, $Mg_{0.2}H_{0.6}$; 6, $Mg_{0.21}Al_{0.16}$; 7, $Zn_{0.2}Li_{0.6}$; 8, $Zn_{0.2}H_{0.6}$; 9, $Zn_{0.21}Al_{0.16}$; 10, $Mg_{0.5}$; 11, $Zn_{0.5}$.

Accuracies for the dehydrated forms are severely affected by considerable line broadening that indicates a highly defective structure. For $LiAlSi_2O_6$, $Mg_{0.5}AlSi_2O_6$ and $Zn_{0.5}AlSi_2O_6$ the lattice constants given here are in agreement with literature data within the limits of error. Table III also contains thermal expansion data calculated from lattice constants refined for the temperatures indicated. For the temperature range investigated here thermal expansion coefficients are constant within the limit of accuracy given.

The variation of lattice constants for the keatite-phases is shown graphically in Fig. 2. The substitution of Mg^{2+} or Zn^{2+} for $2Li^+$ has only minor consequences for the keatite lattice constants. In contrast, there is a substantial shrinkage of the c-axis upon replacement of Li^+ by H^+, namely by $\sim 8\%$ in pure $HAlSi_2O_6$. The c-axis shrinkage is commensurately less pronounced in the magnesium- and zinc-containing keatites. The dehydrated keatites have c-dimensions somewhere in between the corresponding lithium and hydrogen forms. Changes in the a-axis are much less pronounced, but it may be seen that incorporation of Mg^{2+} as well as dehydration tend to slightly shorten the a-axis. Fig. 2 also shows the variation of lattice constants on heating. The length and direction of the lines represents the thermal changes. For ease of comparison all data from Table III have been normalized to the 25 to 800° C range even though the hydrogen-containing phases are stable only up to $\sim 450°$ C. The predominant thermal feature in all keatite phases is an increase in the c-axis, which is strongest in the hydrogen-containing phases and weakest in the dehydrated ones. The a-axis tends to decrease thermally in phases with high lithium and zinc components and to increase in all others.

Fig. 3 represents the lattice constants and thermal variations for the β-quartz phases. Here, leaching again leads to volume shrinkage, though the effect is not as pronounced as in the keatite phases, due to a shortening of the a-axis. The lattice geometry of the magnesium-containing β-quartz phase differs markedly from that of the lithium- and zinc-containing ones, with Mg^{2+} ions contracting both the a- and c-axes. Dehydration apparently has somewhat similar consequences on lattice geometry as magnesium incorporation. The thermal effects in all phases except those rich in lithium and zinc are dominated by an a-axis increase. The c-axis decreases strongly in the lithium- and zinc-rich phases, but only slightly in the others. High magnesium contents again apparently counteract this trend.

3.4. Reversibility and intermediate states

The exchange reaction 1 can be reversed both by diffusion and electrolysis. Thus, by immersion in molten $LiNO_3$ at $\sim 300°$ C for 5 h both keatite- and β-quartz-$LiAlSi_2O_6$ are readily formed from their respective hydrogen forms. The same result is obtained by solid state electrolysis of pressed $HAlSi_2O_6$ (keatite or β-quartz) pellets between LiCl pellets. Typical conductivities of the $HAlSi_2O_6$ phases vary from $\sim 2 \times 10^{-8}\,\Omega^{-1}\,cm^{-1}$ at 200° C to $\sim 3.6 \times 10^{-7}\,\Omega^{-1}\,cm^{-1}$ at 300° C, giving an activation energy ~ 0.7 eV for the conduction process. Conductivity does not vary appreciably with time and is also about the same in pure

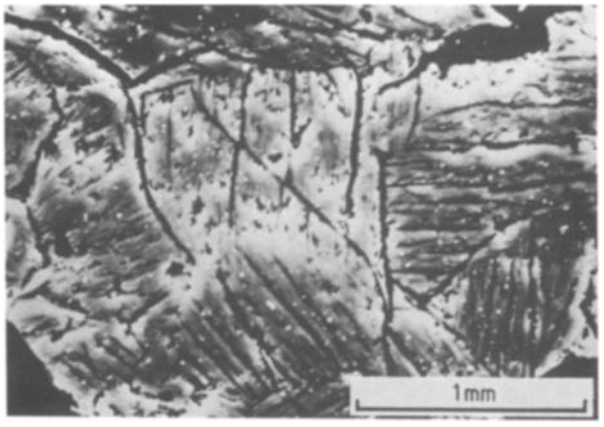

Figure 4 Scanning electron micrograph of $HAlSi_2O_6$ (keatite) polycrystal showing parallel cracks formed during Li–H exchange.

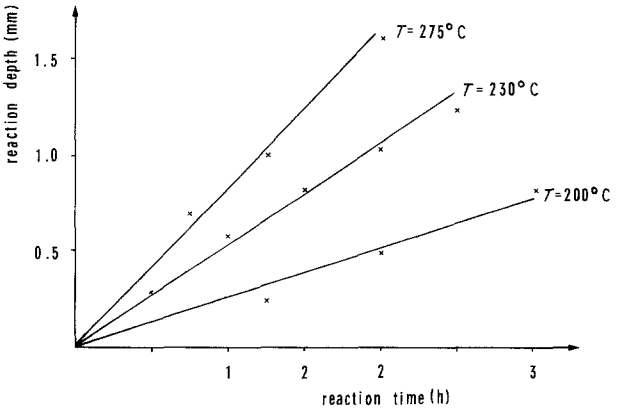

Figure 6 Reaction depth of Li–H exchange in polycrystalline $LiAlSi_2O_6$ (keatite) aggregates as a function of time and temperature in 98% H_2SO_4.

$LiAlSi_2O_6$ samples. The integral charge (current × time) required for complete regeneration of $LiAlSi_2O_6$ from the hydrogen form is roughly compatible with Faraday's law. This indicates that lithium and hydrogen are the dominant charge carriers and it can also be concluded that their mobilities are about the same.

Neither diffusion nor electrolysis experiments yielded indications of the formation of solid solutions of the type (Li, H)$AlSi_2O_6$. Also, leaching experiments with excess amounts of $LiAlSi_2O_6$ always yielded two-phase products approaching the cell geometries of pure $LiAlSi_2O_6$ and $HAlSi_2O_6$. The dehydration apparently is not reversible: neither treatment of the dehydrated form in steam nor immersion in molten LiCl had any effect on lattice geometry or composition.

3.5. Morphology of the leached and dehydrated phases

Grossman and Lanning [2] described the microstructure of leached and dehydrated keatite-type ceramic bodies in detail. They especially emphasized the formation of systems of parallel cracks during leaching. These cracks have also been noticed in all bulk specimens of leached keatite phases in the present study, see Fig. 4. They do not form, however, in sufficiently small, isolated grains. Upon dehydration the cracks partially heal and close again, as documented in Fig. 5. In β-quartz-$LiAlSi_2O_6$ crack formation is much less pronounced, probably due to the smaller unit cell contraction during leaching.

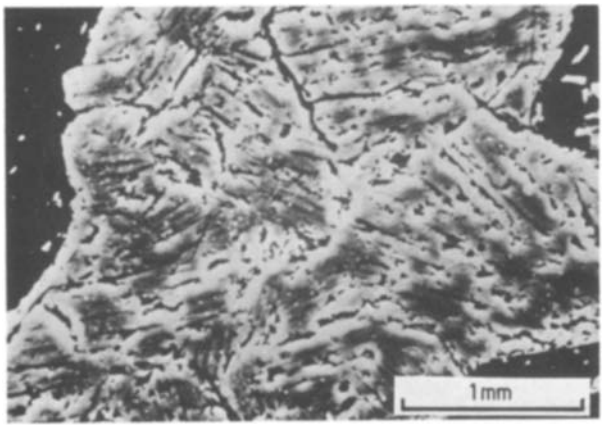

Figure 5 Scanning electron micrograph of dehydrated keatite polycrystal showing that parallel cracks have partially healed.

3.6. Kinetics of the leaching reaction

Due to the formation of the cracks, the depths of the leached zone can readily be measured optically in dense, polycrystalline $LiAlSi_2O_6$-keatite bodies: the cracks cause a characteristic whitish opalescence in the reacted zone which is absent in the unreacted core. The reaction depths as a function of time and temperature as represented in Fig. 6 have been measured in this way. The thickness of the reacted rim seems to vary linearly with time which indicates that the reaction rate is not diffusion controlled. It is assumed that the cracks provide access of the sulphuric acid to the reaction front thus eliminating the need for long-range volume or surface diffusion of the reactants.

From Fig. 6 a gross activation energy of about 0.22 eV can be deducted. This energy is much smaller than the activation energy found for the electrical conductivity, which again shows that solid-state diffusion is not the limiting factor for the overall reaction rate.

4. Discussion

4.1. The structural chemistry of leaching and dehydration processes

As has been shown above for both the keatite- and β-quartz type aluminosilicates, neither the leaching nor the dehydration process affects apparent space group symmetry. The lattice constants do vary appreciably indicating considerable deformation of the framework, to a degree that prevents the formation of solid solutions between the lithium and the hydrogen forms. Mixed cation solid solutions are accessible, though, by substitution of magnesium and zinc ions for lithium ions, due to the immobility of the divalent ions at the low temperatures of the leaching process. From these solid solutions it can be seen that the cell geometry apparently varies continuously with cationic (the cations including H^+ in this discussion) composition. All this indicates that the structural coherency of the framework is fully maintained during leaching. This is further supported by the straightforward reversibility of the reaction.

The leaching reaction can thus, in agreement with

all analytical data, be described as a reversible cation exchange of Li^+ against H^+, that obviously leads to considerable distortions of the framework, yet does not affect its linkage.

Cation exchange under mild conditions is a typical phenomenon for zeolites. Indeed, zeolites containing hydrogen as the major cationic species have variously been described (e.g. [13]). The protons there are bonded to framework oxygens, thus forming bridging hydroxyl ions. The same structural concept is suggested here for the $HAlSi_2O_6$ and related phases. The geometry of the bridging OH ions in zeolites is such that the proton is located about 0.1 nm from the oxygen in the plane defined by the Al,Si–O–Al,Si bonds, pointing away from the framework cations. In this way the protons point into the rather spacious cages of the zeolite structures. The keatite- and β-quartz structures, in contrast, do not have any comparable cages but only voids accommodating ions the size of Li^+, Mg^{2+} or Zn^{2+}, i.e. up to ~ 0.08 nm. If the zeolite model of the bridging OH-ions is adopted for these structures, then the protons come into close vicinity (~ 0.2 to 0.25 nm) with other oxygen ions, which would suggest the formation of hydrogen bonds.

Symmetry conservation and lattice constant variation indicate that the structural linkage is also maintained during dehydration. The structural transition must be complicated, though, due to the removal of framework oxygen during dehydration. The observed X-ray line broadening is indicative of the defects caused by this – at least temporary – disruption of the framework. The analogous process in zeolites is again well documented, the result being a transition of aluminium ions from framework positions into some non-framework species, which results in de-alumination of the framework [13]. Yet the framework is reconstituted into the old linkage. The structural formulae presented in Table III reflect this model-dealumination of the framework and maintenance of the charge balance by non-framework aluminium ions. In the next section it will be shown that the lattice constants and thermal expansion data indeed support such a model.

4.2. Comparison of hydrogen and other cations in the keatite- and β-quartz aluminosilicates

In the keatite and β-quartz structures of $LiAlSi_2O_6$ [4–6] the lithium ions occupy voids with irregular tetrahedral coordination of oxygen. Both frameworks have disordered Al/Si distributions. In β-quartz-$Zn_{0.5}AlSi_2O_6$ the zinc ions predominantly occupy the same positions as the lithium ions [14]. This is in contrast to the results obtained on $MgAl_2Si_3O_{10}$, another member of the β-quartz series of solid solutions: the magnesium ions here at least predominantly occupy positions with irregular octahedral coordination [11]. The coordination of magnesium and zinc ions in keatite solid solutions is not as well established, but strong indications have been presented that in these phases magnesium ions adopt the same type of tetrahedral coordination as lithium ions [10]. The close similarity in cell dimensions and thermal expansion evidenced in Fig. 2 supports this view and also suggests that zinc ions occupy the same positions – in agreement with the general preference of zinc for tetrahedral oxygen coordination.

In the β-quartz structure, both the tetrahedral and the octahedral cation positions are located in the channels running parallel to the c-axis. As can be seen from Fig. 3, the a-axis is longest for the phases with tetrahedrally coordinated cations. Incorporation of the octahedrally coordinated magnesium ions contracts both the a- and c-axis. The hydrogen form has the smallest a-axis and largest c-axis of all, which in the zeolite-derived model described above is reasonable, because any hydrogen bonds would link oxygens of equal z-coordinate and thus leave the c-direction unaffected. Lattice constants of the dehydrated form are about halfway between the magnesium and the hydrogen form. As has been noted in similar systems [15], thermal expansion of framework aluminosilicates tends to counteract the effects of chemical substitutions on framework geometry. This trend can be seen in Fig. 3 also, with the magnitude of the thermal effects being larger for the univalent cations than for the divalent ones. The notion that trivalent aluminium ions provide the charge balance in the dehydrated phases fits into this picture.

In the keatite structure, where lithium, magnesium and zinc ions occupy the same crystallographic positions, their respective lattice geometries and thermal effects are very similar. This reflects the similar size of these ions and also implies that the smaller number of the divalent ions per unit cell is compensated by their higher bond strength. In the β-quartz structure the particular role of magnesium ions as compared to lithium and zinc ions can be explained by their preference for octahedral coordination. Aluminium ions are much smaller than lithium, magnesium and zinc. Thus substitution of aluminium ions should lead to reduced cell volume. In the keatite phase, this is clearly the case. In the β-quartz phase the cell volume is similar to that of the magnesium containing phase, but lattice constants differ markedly. This seems to suggest that the coordination of magnesium and aluminium in these phases may not be the same, as might be expected. Single crystal work is obviously needed here.

Hydrogen has very different oxygen coordination, namely one, or in the case of hydrogen bonding, two. Neither case requires extra volume to accommodate the H^+ ions. The shortest oxygen–oxygen distances outside the $(Al, Si)O_4$ tetradra are the most likely positions for hydrogen bonding. These lie in the c-direction in keatite and in the a_1–a_2 plane in β-quartz. The corresponding cell edges are exactly those being drastically shortened in the hydrogen forms, whereas the remaining ones, that would be unaffected by hydrogen bonding, actually become longer on H^+ incorporation.

5. Conclusions

It has been shown that leaching of keatite- and β-quartz-type lithium-aluminosilicates by hot concentrated acids can be described as an Li–H exchange,

that can be reversed and does not affect the linkage of the framework. Dehydration of the hydrogen forms is irreversible and causes considerable lattice defects, but still leaves the framework linkage unaltered. Dealumination of the framework and formation of non-framework, charge balancing Al^{3+} cations is suggested as the mechanism of the dehydration reaction.

Acknowledgement

This work was supported by Deutsche Forschungs-Gemeinschaft, which is gratefully acknowledged.

References

1. R. B. ELLESTAD and K. M. LEUTE, US Patent 2 516 109 (1950).
2. D. G. GROSSMAN and J. G. LANNING, *Ceram. Bull.* **56** (1977) 474.
3. Y. J. OSTROUSHKO, K. J. FILIPPOVA and L. A. IGNAT'EVA, *Russ. J. Inorg. Chem.* **7** (1962) 126.
4. C. T. LI and D. R. PEACOR, *Z. Kristallogr.* **126** (1968) 46.
5. C. T. LI, *ibid.* **127** (1968) 327.
6. P. T. CLARKE and J. M. SPINK, *ibid.* **130** (1969) 420.
7. W. SCHREYER and J. F. SCHAIRER, *ibid.* **116** (1961) 60.
8. J. PETZOLD, *Glastech. Ber.* **40** (1967) 358.
9. S. RAY and G. M. MUCHOW, *J. Amer. Ceram. Soc.* **51** (1968) 678.
10. S. RAY, *ibid.* **54** (1971) 213.
11. H. SCHULZ, W. HOFFMANN and G. M. MUCHOW, *Z. Kristallogr.* **134** (1971) 1.
12. G. H. BEALL, B. R. KARSTETTER and H. L. RITTLER, *J. Amer. Ceram. Soc.* **50** (1967) 181.
13. R. X. FISCHER, W. H. BAUR, R. D. SHANNON, R. H. STALEY and A. J. VEGA, *Fortschr. d. Mineralogie* **54** (1986) Beiheft 1: 49.
14. M. BEHRUZI and T. HAHN, *ibid.* **55** (1977) Beiheft 1: 12.
15. G. MÜLLER, *ibid.* **63** (1985) 7.

Received 16 July
and accepted 9 October 1987